PERGAMON

Control Engineering Practice 6 (1998) 359–367

Robust digital friction compensation

Min Sig Kang*

1-1-4, Agency for Defense Development, P.O. Box. 35, Yusung, Daejon, Korea

Received January 1997; accepted December 1997

Abstract

Even though the nonlinear compensator proposed by Southward, et al. can guarantee the closed-loop stability for stick-slip friction systems in continuous-time control, applying this to digital control systems may often generate a limit cycle response in the vicinity of a reference position because of the inherent time delay of sample-and-hold operation. In this paper, a new robust digital friction compensator (RDFC) is proposed, which consists of a digital P controller + hysteresis friction compensator part (position feedback loop) and an analog D controller part (velocity feedback loop). The hysteresis compensator in the position feedback loop increases the phase lead in comparison with Southward's technique such that the phase lag coming from the time delay of digital control can be compensated for. A modified form of Lyapunov's stability theorem is employed to verify the asymptotic stability of the RDFC. Stability and control effectiveness are verified analytically and experimentally on a single-axis robot system.

Keywords: Stick-slip friction, limit cycle, hysteresis compensators, steady-state position errors, time delay, phase lead/lag

1. Introduction

Stick-slip friction is a commonly encountered phenomenon in mechanical systems. The effect of friction on machines is noticeable at very low velocities. At these speeds, motion tends to be intermittent. Commonly referred to as stick-up, intermittent motion can lead to overshoot and large-amplitude position or force limit cycling.

Various friction compensation techniques that are effective in ameliorating the effect at low velocities have been proposed for a servo mechanism to perform regulation tasks (Amstrong et al., 1994). These are high-gain PD control, PID control, feedforward compensation (Brandenburg and Schafer, 1989), adaptive control (Yang and Tomizuka, 1988; Canudas et al., 1987), etc. For regulation problems, high-gain PD control can reduce the steady-state position error, but often causes system instability when the drive train is compliant (Dupont, 1994; Dupont and Dunlap, 1995). PID control may promote the generation of limit cycles, thus resulting in motion intermittence (Radcliff and Southward, 1990; Armstrong and Amin, 1996).

One of the techniques to alleviate the steady state position error and the destabilizing effect of the friction is the robust non-linear friction compensation proposed by Southward et al. (1991). This technique introduces a specific non-linear compensation force that supplements a standard PD control force. As a result, the asymptotic stability of the desired reference position is guaranteed for the stick-slip friction system. This control is easily applicable to practical systems because it is a non-model-based scheme, and a robust one; it does not require the exact friction model, which is difficult to obtain in practice, but requires only the upper bounds of the static friction levels; it is robust with respect to the characteristics of the slipping force, which is assumed to lie within a piecewise linear band (Southward et al., 1991).

The non-linear friction compensation so far has been studied in continuous time; it has not been addressed in discrete time. Since controllers are usually implemented by digital computers, discrete-time compensation design is an important consideration. Due to the sample-and-hold operations, discrete-time control induces an inherent time delay in comparison with continuous-time control. In general, time delays degrade a system's stability. Motivated by this time delay, this work investigates the instability of Southward's technique in digital control systems, and suggests a new technique that can guarantee the asymptotic stability of the digital control of stick-slip

* Present address: Department of Mechanical Design and Production Engineering, Kyungwon University, Bokjung-Dong, Sujung-Gu, Songnam, Kyunggi-Do, Korea. E-mail: mskang@sunam.kreonet.re.kr

0967-0661/98/$19.00
PII S0967-0661(98)00008-2

friction systems. This technique is also a non-model-based scheme. So, no knowledge of the slipping friction is required, and only the upper bounds of the static friction levels are needed. The slipping friction is assumed to lie within a piecewise linear band.

The friction model to be discussed is represented in Section 2, and Southward's technique is briefly reviewed in Section 3. In Section 4, the instability of Southward's technique when applied to digital control systems is analyzed and proved. In Section 5, a new hysteresis friction compensation is suggested, and its asymptotic stability is proved analytically. By using the stabilization effect of the hysteresis compensator, a robust digital nonlinear friction compensation is proposed. Finally, in Section 6, the techniques mentioned above are applied to a single-axis robot system, and experimental results are discussed.

2. Friction model

Consider a 1-DOF robot system described by the differential equation

$$\begin{aligned} J\ddot{\theta} &= -T_d + T_c \\ \omega &= \dot{\theta} \end{aligned} \tag{1}$$

which relates the rotation angle θ of the rotor of inertia J to the stick-slip friction torque, T_d and the control torque T_c. The friction torque can be represented by the sum of the static torque, T_{stick}, and the slippling torque, T_{slip} (Karnoop, 1985). The static torque corresponds to the resistive torque at zero velocity, and its positive and negative limits are given by T_s^+ and T_d^-, respectively. The magnitudes of T_s^+ and T_s^- are not presumed equal.

$$T_{stick} = \begin{cases} T_s^+ & 0 < T_s^+ < T_c \\ T_c & T_s^- \leqslant T_c \leqslant T_s^+ \\ T_s^- & T_c < T_s^- < 0 \end{cases} \tag{2}$$

The slipping torque provides the torque at nonzero velocity, and is represented by

$$T_{slip}(\omega) = T_d^+(\omega)\mu(\omega) + T_d^-(\omega)\mu(\omega) \tag{3}$$

where $\mu(\cdot)$ is the right-continuous Heaviside step function. The function $T_d^+(\omega)$ is the slipping torque for positive velocities, and the fucntion $T_d^-(\omega)$ is the slipping torque for negative velocities. The magnitudes of $T_d^+(\omega)$ and $T_d^-(\omega)$ are not presumed to be symmetrical. The slipping torque is assumed to be bounded within the first and third quadrants.

$$\begin{aligned} b_0\omega \leqslant T_d^+(\omega) \leqslant T_0^+ + b_1\omega, \quad \forall\omega > 0 \\ T_0^+ + b_1\omega \leqslant T_d^-(\omega) \leqslant b_0\omega, \quad \forall\omega < 0 \end{aligned} \tag{4}$$

where it is assumed that there exist constants $b_1 \geqslant b_0 > 0$, $T_s^+ \geqslant T_0^+ > 0$, and $T_s^- \leqslant T_0^- < 0$.

3. Southward's nonlinear friction compensation

For the system given in Eqs. (1)–(4), under PD control, all trajectories end up at a point within the equilibrium region, E_{PD}, defined by

$$E_{PD} = \{(\theta, \omega) | \omega = 0, \theta_L \leqslant \theta - \theta_R \leqslant \theta_H\} \tag{5}$$

where θ_R denotes the reference input position and

$$\theta_L = -\left(\frac{T_s^+}{K_p}\right) < 0, \quad \theta_H = -\left(\frac{T_s^-}{K_p}\right) > 0. \tag{6}$$

Thus, traditional PD control results in a steady-state position error (Radcliff and Southward, 1990).

The nonlinear friction compensation introduced by Southward et al. (1991) eliminates the steady-state position error and guarantees the asymptotic stability of a desired reference position for the system given in Eq. (1) in the presence of stick-slip friction modeled by Eqs. (2)–(4). The control is given as

$$T_c = -K_d\omega - T_n \tag{7}$$

where K_d is the derivative control gain, and T_n is the discontinuous nonlinear friction compensation torque which supplements a standard PD control torque.

$$T_n = \begin{cases} -\tilde{T}_s^- & 0 < \theta \leq \tilde{\theta}_H \\ 0 & \theta = 0 \\ -\tilde{T}_s^+ & \tilde{\theta}_L \leq \theta \leq 0 \\ K_p\theta & \text{otherwise} \end{cases} \tag{8a}$$

where

$$\begin{cases} \tilde{\theta}_H = \theta_H + \varepsilon \\ \tilde{\theta}_L = \theta_L - \varepsilon, \ \varepsilon > 0 \end{cases} \tag{8b}$$

$$\begin{cases} \tilde{T}_s^+ = -K_p\tilde{\theta}_L = T_s^+ + K_p\varepsilon \\ \tilde{T}_s^- = -K_p\tilde{\theta}_H = T_s^- - K_p\varepsilon \end{cases} \tag{8c}$$

The nonlinear compensation torque is only active when the rotor is between the extended sticking limits $\tilde{\theta}_L \leq \theta \leq \tilde{\theta}_H$. When the rotor is within this region, any positive value of ε is enough to ensure that the feedback torque exceeds the static friction, and thus the rotor moves continuously towards the origin.

Notice that this controller is essentially a PD controller outside the nonlinear control region θ_n defined by $\theta_n \equiv \{\tilde{\theta}_L \leq \theta \leq \tilde{\theta}_H\}$.

3.1. Instability of Southward's technique for digital control systems

Even though Southward's technique guarantees the asymptotic stability of continuous-time control systems, this technique induces a stable limit cycle response in

digital control systems. In this section, this instability is proved analytically by using the Lyapunov instability theory. The basic conceptual explanation of the occurrence of the limit cycle response is as follows.

Consider a displacement that has to be fed back, represented by a harmonic function $\theta(t)$ that is assumed to be bounded by $\tilde{\theta}_L$ and $\tilde{\theta}_H$ (see Fig. 1). Then, from Eq. (8), the compensation torque $-T_n$ will be given by the solid line. It is a bang-bang torque, and has the opposite sign from $\theta(t)$. If Southward's technique is applied to a digital control system, it can be assumed that $\theta(t)$ is sampled at $t = \ldots, kT, (k+1)T, \ldots, nT, (n+1)T, \ldots$ as given in Fig. 1, where T denotes the sampling interval. The k'th (or n'th) and $(k+1)$'th (or $(n+1)$'th) sampling instants correspond to the nearest one before $\theta(t)$ approaches zero, and the one after $\theta(t)$ departs from zero, respectively. Without any loss of generality, the sampling instants do not coincide exactly with the time at which $\theta(t)$ is identically zero. Thus the compensation torque, $-T_n$, sustains the previous value at the time $t = kT$ (or $t = nT$) until the time $t = (k+1)T$ (or $t = (n+1)T$) as denoted by the dotted line. This implies that the digital implementation of Southward's technique induces an additive time delay in comparison with the continuous-time application of the technique. This time delay arises from the sample-and-hold operation of digital controls. During a control process, this time delay is not deterministic because it depends on the sampling period and the system responses. However, this time delay always exists and does not exceed the sampling period. It is obvious from Fig. 1 that the compensation torque in the periods defined by $\Delta_k T$ and $\Delta_n T$ accelerates the response because the control input has the same direction as the velocity of the response. Therefore, the origin of the state space is no longer stable.

Based on the above discussion, the friction compensation torque T_n in digital controls can be represented equivalently by Eq. (9) (See Fig. 2).

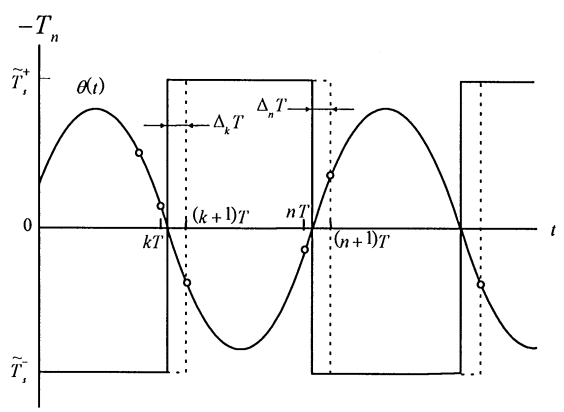

Fig. 1. Nonlinear compensation torque of Southward's technique in continuous and digital control systems (solid: continuous, dotted: digital).

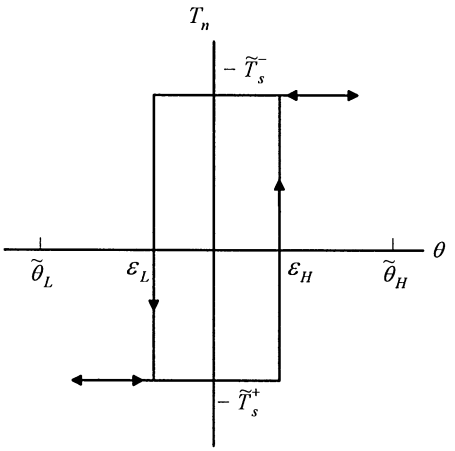

Fig. 2. Equivalent compensation torque of the Southward control in digital control systems.

(i) When $\omega > 0$

$$T_n = \begin{cases} -\tilde{T}_s^- & \varepsilon_H < \theta < \tilde{\theta}_H \\ -\tilde{T}_s^+ & \tilde{\theta}_L < \theta \le \varepsilon_H, \end{cases} \tag{9.1}$$

(ii) when $\omega < 0$

$$T_n = \begin{cases} -\tilde{T}_s^- & \varepsilon_L < \theta < \tilde{\theta}_H \\ -\tilde{T}_s^+ & \tilde{\theta}_L < \theta < \varepsilon_L. \end{cases} \tag{9.2}$$

For simplicity, the control is considered only in the nonlinear control region θ_n. It is enough to discuss the instability of the origin. Nonzero ε_H and ε_L stand for the qualitative effect of a nonzero time delay. Note that a quantitative conversion of the time delay to the equivalent ε_H and ε_L is not possible, but the fact that ε_H and ε_L are not zero is sufficient to prove the instability of Southward's technique when applied to digital control systems.

Consider the system represented by Eqs. (1)–(4) under the control given by Eqs. (7) and (9). Since the slipping friction is discontinuous at $\omega = 0$, and the applied control torque T_c is essentially discontinuous, the system (1) has the surface of discontinuity S_1, defined as

$$S_1 = [(\theta, \omega) | \{\omega = 0\} \cup \{\theta = \varepsilon_H, \omega > 0\} \cup \{\theta = \varepsilon_L, \omega < 0\}]. \tag{10}$$

Theorem 1. *The origin of the state space for the system given by Eqs.* (1)–(4), *with the control given by Eqs.* (7) *and* (9), *is unstable.*

The proof is given in Appendix A.

This instability analysis is discussed only in the nonlinear control region θ_n. In the linear control region, outside θ_n, the closed-loop system is stable as long as the proportional gain, K_p, and the derivative gain, K_d, are designed reasonably. Therefore the system will exhibit a stable limit cycle response.

4. Hysteresis nonlinear friction compensation

To eliminate the instability of the Southward compensation in the digital control of stick-slip friction systems, a hysteresis nonlinear compensation technique is proposed, and the stability is discussed in this section.

The control has the same form as in Eq. (7):

$$T_c = -K_d\omega - T_n, \tag{11}$$

but the nonlinear friction compensation T_n is the hysteresis function as given by (12) (see Fig. 3).

(i) When $\omega > 0$

$$T_n = \begin{cases} -\tilde{T}_s^- & 0 < \theta \le \tilde{\theta}_H \\ 0 & \delta_L \le \theta \le 0 \\ -\tilde{T}_s^+ & \tilde{\theta}_L \le \theta \le \delta_L \\ K_p\theta & \text{otherwise,} \end{cases} \tag{12a}$$

(ii) when $\omega < 0$

$$T_n = \begin{cases} -\tilde{T}_s^- & \delta_H < \theta \le \tilde{\theta}_H \\ 0 & 0 \le \theta \le \delta_H \\ -\tilde{T}_s^+ & \tilde{\theta}_L \le \theta \le \delta_L \\ K_p\theta & \text{otherwise,} \end{cases} \tag{12b}$$

(iii) when $\omega = 0$

$$T_n = \begin{cases} -\tilde{T}_s^- & \delta_H < \theta \le \tilde{\theta}_H \\ 0 & \delta_L \le \theta \le \delta_H \\ -\tilde{T}_s^+ & \tilde{\theta}_L \le \theta \le \delta_L \\ K_p\theta & \text{otherwise,} \end{cases} \tag{12c}$$

where the parameters $\tilde{\theta}_H$ and $\tilde{\theta}_L$ are the same as in Eq. (8b). The parameters δ_H and δ_L are nonzero constants, to be designed, and those denote the bounds of the velocity-dependent dead zone. It is assumed that $\tilde{\theta}_L < \delta_L$ and $\delta_H < \tilde{\theta}_H$. When the rotor approaches the zero position, the nonlinear compensation torque, T_n, is set to be zero from just after the trajectory enters into the dead zone until it leaves the dead zone. Applying properly designed dead bounds in the consideration of the time delay, T_n can be made to be zero during the periods $\Delta_k T$ and $\Delta_n T$ in Fig. 1. Thus the compensator given by Eq. (12) can eliminate the destabilizing effect of the time delay.

Theorem 2. *The region* S_δ, $S_\delta = \{(\theta, \omega) | \delta_L \le \theta \le \delta_H, \omega = 0\}$, *is an asymptotically stable equilibrium set of points for the system given by Eqs.* (1)–(4) *with the control given by Eqs.* (11) *and* (12).

The proof is given in Appendix B.

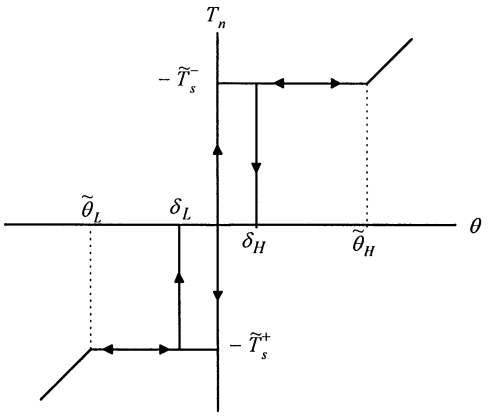

Fig. 3. Hysteresis friction compensation.

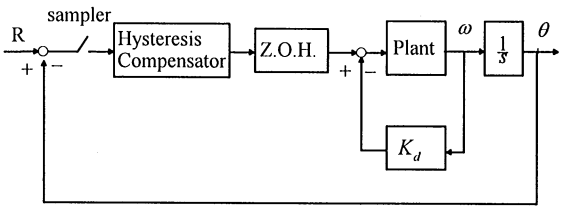

Fig. 4. Robust digital friction compensation.

From describing function analysis (Olsson, 1995), this hysteresis compensator obviously increases the phase lead in comparison with the continuous-time application of Southward's technique. This phase lead can compensate for the phase delay that comes from the time delay in digital control systems. By utilizing this phase lead property of the hysteresis compensator, a new friction-compensation technique, known as the robust digital friction compensator (RDFC), is proposed. As shown in Fig. 4, the RDFC consists of a digital P + hysteresis friction compensator part (position feedback loop) and an analog D-controller part (velocity feedback loop). The stability of the RDFC depends on the sampling interval, δ_H and δ_L, and the amount of the excessive levels of $\tilde{T}_s^+$ and $\tilde{T}_s^-$ in the real static friction levels. It should be noticed that, this RDFC results in steady-state position errors bounded by δ_H and δ_L, because all points in S_δ are stable equilibrium ones.

Remarks

1. As the magnitudes of δ_H and δ_L increase, the amount of phase lead also increases monotonically, up to 0.5π radians; thus there always exist δ_H and δ_L for a given sampling interval such that the destablizing effect of the digital control can be eliminated.
2. Since the extreme value of the time delay in the position feedback-loop is equal to the sampling interval T, a set of parameters δ_H and δ_L, designed for the system with time delay T, guarantee the asymptotic stability of the RDFC.

3. Analytical design of δ_H and δ_L is not easy, so they can be designed through a describing function analysis and simulation studies.
4. Increasing the magnitude of δ_H and δ_L improves the stability margin, but, on the other hand, it means enlarging the possible position error bounds. Therefore, a compromise must be found between the stability margin and the positioning accuracy.
5. Faster sampling is advantageous in terms of improving the stability margin and the positioning accuracy, because faster sampling means smaller time delays.

6. Experiments

Experiments have been performed with a single-axis robot system. The experimental apparatus for the purpose of confirming the results discussed in the previous sections consists of a rotor supported by a ball bearing, a DC servo motor connected with a harmonic drive with a 1/100 reduction ratio, a servo amplifier with a current feedback loop, an encoder of the resulting rotor position with resolution 2.44×10^{-6} deg, and a PC-486DX equipped with a DSP board on which 12-bit D/A converter and an encoder interface are placed. The moment of inertia reflected to the rotor axis is determined to be 0.0212 Nm sec^2/deg. The schematic diagram of the experimental set-up is shown in Fig. 5. An analog velocity feedback is realized by using the tachometer connected to the rotor.

To estimate the maximum static torque, P-control is realized in the DSP board, and a simple ramp function is selected as the reference position input. A positive reference input is assigned to the clockwise direction.

Throughout these experiments for system identification, the sampling time is kept at 5 ms. Fig. 6a shows the slowly increasing reference input in the form of a ramp and the resulting rotation angle. The applied control torque is given in Fig. 6. These reveal stick-slip motion. During sticking, the control torque rises and reaches the level of static friction, and slip begins. During slip, the control torque decreases rapidly and the rotor is arrested. These stick and slip cycles are then repeated.

Since the static friction torque, which is measured by the control torque at the breakaway point from rest to

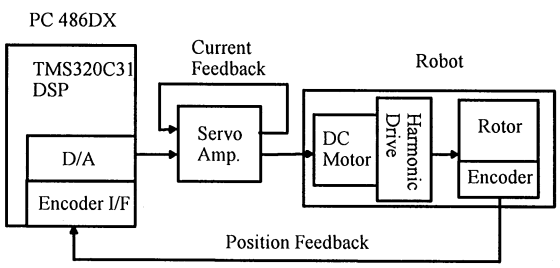

Fig. 5. Schematic diagram of the experimental setup.

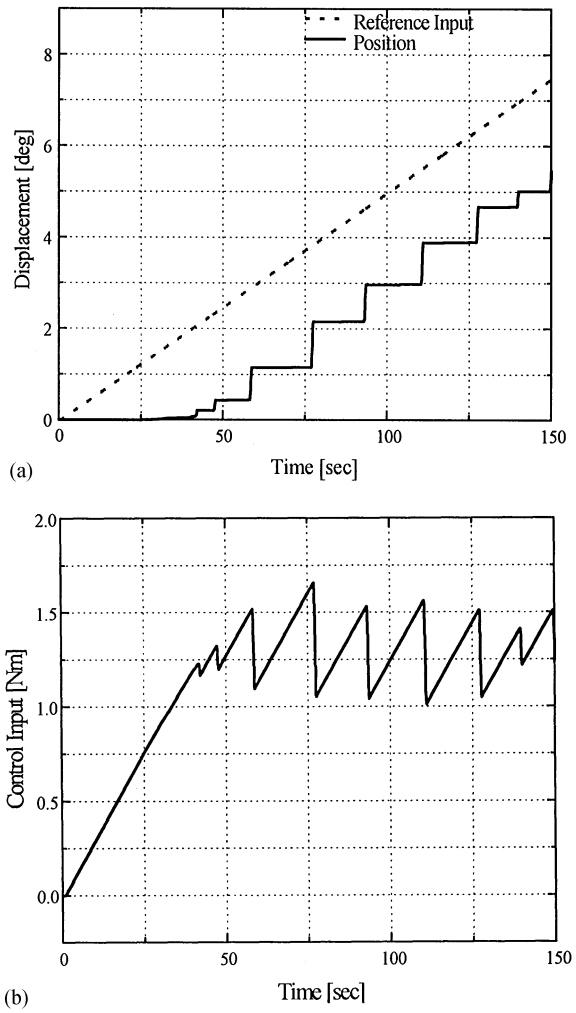

Fig. 6 (a) Reference input and stick-slip response. (b) Control input with stick-slip motion.

slipping, decreases as the slope of the reference input and the P-gain increase, a very slowly increasing reference input of 0.05 deg/sec is chosen to obtain its maximum level (Canudas et al., 1995). The control torque to the other reference inputs, slower than 0.05 deg/sec, shows only a very little difference compared to Fig. 6b. As can be seen in Fig. 6b, the maximum static friction torque is not uniform, but position-dependent. Since the upper bounds of the maximum static friction torques are required for the design of the nonlinear friction compensators, the maximum value of the maximum control torques is selected as the positive maximum static friction torque. That is determined to be $\tilde{T}_s^+ = 1.785$ Nm. Similar experiments are carried out in the counterclockwise direction and the negative maximum static friction torque, $\tilde{T}_s^-$, is determined to be -1.441 Nm. The clockwise direction involves more sticking than the reverse direction.

The slipping friction is relatively complicated to model. In this experiment, it was assumed that slipping

torque can be modeled as a linear combination of Coulomb and viscous torques. Accurate modeling of the slipping friction is relatively unimportant in these experiments, because only the maximum values of the static friction levels are needed to design the controllers. From various experiments, the Coulomb torques, $\tilde{T}_0^+$ and $\tilde{T}_0^-$, and the viscous friction coefficients, c^+ and c^-, are determined to be $\tilde{T}_0^+ = 1.26$–1.32 Nm, $\tilde{T}_0^- = -0.95$–0.97 Nm, $c^+ = 0.011$–0.020 Nm sec/deg, and $c^- = 0.010$–0.017 Nm sec/deg, respectively. The superscripts "+" and "−" denote the clockwise and the counterclockwise directions, respectively. These terms are all position- and speed-dependent.

A PD-control is applied to test its effect. Throughout the control experiments, the sampling time is kept at 20 ms. The proportional and the derivative gains are chosen to be $K_p = 0.0066$, $K_d = 0.0033$ such that the closed-loop system (ignoring the static and Coulomb frictions) has a damping factor $\zeta = 0.79$–0.87 and the natural frequency $\omega_n = 0.5$ Hz. Using the proportional gain and the estimatiod maximum static torque, the bounds of the equilibrium region, E_{PD}, are determined to be $\theta_H = 6.97$ deg, $\theta_L = -8.64$ deg, respectively. Fig. 7 shows the time response of this PD-control, subject to the initial conditions $\theta(0) = 20$ deg, $\omega(0) = 0$. As expected, the closed-loop response is stable but the steady-state position error does not converge to zero. The measured steady-state position error is $e_{ss} = 0.841$ deg. This error lies within the region bounded by θ_H and θ_L.

In order to verify the occurrence of a limit cycle response when Southward's technique is applied to digital control systems, the controller in Eqs. (7) and (8) is tested. The compensation torques $\tilde{T}_s^+$ and $\tilde{T}_s^-$ are selected to be 20% larger than T_s^+ and T_s^-, respectively, i.e., $\tilde{T}_s^+ = 1.2\ T_s^+ = 2.136$ Nm, $\tilde{T}_s^- = 1.2\ T_s^- = -1.728$ Nm. Therefore the bounds of the nonlinear control region, $\tilde{\theta}_H$ and $\tilde{\theta}_L$, are determined to be 8.36 deg and -10.37 deg, respectively. As discussed in Section 3, the response (subject to the same initial conditions) exhibits a limit cycle response as shown in Fig. 8. From various experiments, it

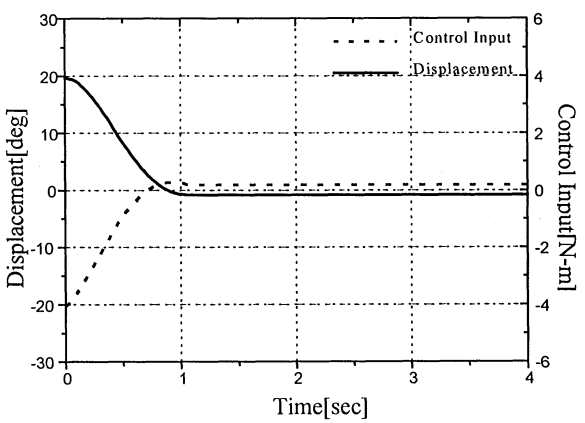

Fig. 7. Time response for PD-control.

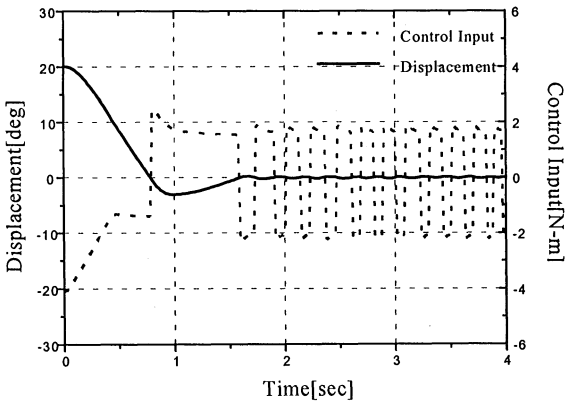

Fig. 8. Time response for Southward's control in a digital control system.

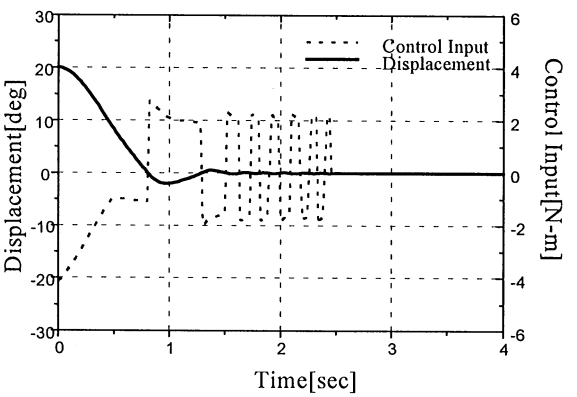

Fig. 9. Time response for RDFC when $\delta_H = -\delta_L = 0.02$ deg.

is confirmed that this control always generates a limit cycle response for any initial condition. As the sampling frequency increases, the amplitude of the limit cycle is decreased because faster sampling reduces the time delay of the original digital control. On the other hand, decreasing the sampling frequency increases the amplitude of the limit cycle.

The experiments were also carried out for the purpose of testing the capability of the RDFC. Fig. 9 shows the response, subject to the same initial conditions. The parameters, δ_H and δ_L, are carefully designed from the describing function analysis and the computer simulation studies to be 0.02 deg and -0.02 deg, respectively. Slightly decreasing the magnitudes of these values will give a stable limit cycle. The start-up transient response is same as that in Fig. 8, but it converges to the steady state after 6 cycles of oscillatory motion. The steady-state position error is measured to be $e_{ss} = 0.007$ deg. This error lies within the region bounded by δ_H and δ_L.

To investigate the effect of δ_H and δ_L, the same experiments are carried out with $\delta_H = -\delta_L = 0.04$ deg. As given in Fig. 10, the period of oscillatory motion is

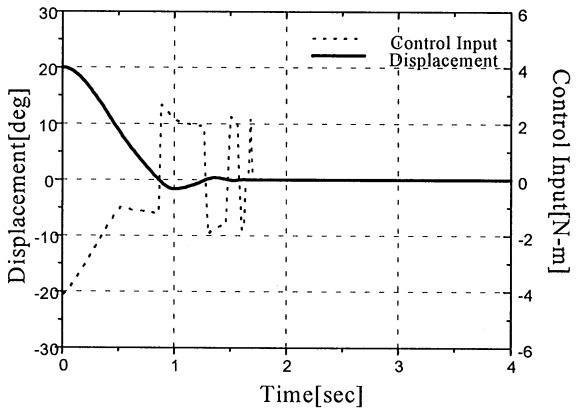

Fig. 10. Time response for RDFC when $\delta_H = -\delta_L = 0.04$ deg.

reduced to 2 cycles, and the steady-state position error is increased; that is, $e_{ss} = 0.023$ deg. The magnitude and the sign of this position error are not consistent because of the uncertainties of the friction. However, it never exceeds the level bounded by δ_H and δ_L. Thus it can be concluded that increasing the absolute values of δ_H and δ_L increases the stability margin, but results in an enlarged possible position error range.

7. Conclusion

In this paper, a new friction-compensation technique employing a hysteresis compensator has been proposed for discrete-time regulating control of a single-DOF servo-system with stick-up friction. The instability of the discrete-time application of the friction compensator proposed by Southward et al. has been verified analytically by using Lyapunov's instability theorem, and has been proved experimentally on a robot system. The hysteresis compensator that is a basic element of the proposed controller leads to an advancement of the phase lead of the closed-loop system in comparison with the continuous-time application of Southward's technique, such that the phase lag coming from the time delays of digital control can be compensated. A modified form of Lyapunov's direct method has been used to prove the asymptotic stability of the closed-loop system. Experimental results have shown the stability and effectiveness of the proposed controller in compensating for the stick-slip friction. Future work will involve the mathematical proof of the stability of RDFC with digital velocity feedback rather than of analog rate feedback, as is common in industrial applications.

Acknowledgements

Thanks are extended to W.G. Song and C.J. Kim and the Agency for Defence Development, KOREA, for their valuable support in the experiments.

Appendix A

Proof of Theorem 1. Choose the Lyapunov function candidate defined in the region θ_n.

$$V_1(\theta, \omega) = (1/2)J\omega^2 + g_1(\theta), \quad \theta \in \theta_n \tag{A.1}$$

where

$$g_1(\theta) = \begin{cases} -\tilde{T}_s^- \theta & 0 \le \theta \le \tilde{\theta}_H \\ -\tilde{T}_s^+ \theta & \tilde{\theta}_L < \theta \le 0. \end{cases} \tag{A.2}$$

From Eqs. (A.1) and (A.2), this Lyapunov function candidate is continuous with respect to θ and ω, and positive definite in the restricted region θ_n. The time derivative of $V_1(\theta, \omega)$ along the system trajectory excluding S_1 is given by

$$\begin{aligned} \dot{V}_1(\theta, \omega) &= J\ddot{\theta} + g_1'(\theta)\omega = \omega(T_c - T_d) + g_1'(\theta)\omega \\ &= \omega(-K_d\omega - T_n - T_d) + g_1'(\theta)\omega \\ &= -K_d\omega^2 - \omega T_{slip}(\omega) + \omega\{g_1'(\theta) - T_n\}, \\ &\quad \forall\theta \in \theta_n, \theta \in S_1 \end{aligned} \tag{A.3}$$

where

$$g_1'(\theta) = \begin{cases} -\tilde{T}_s^- & 0 < \theta < \tilde{\theta}_H \\ \text{undefined} & \theta = 0 \\ -\tilde{T}_s^+ & \tilde{\theta}_L < \theta < 0. \end{cases} \tag{A.4}$$

If $\dot{V}_1(\theta, \omega)$ is positive definite in a certain neighbourhood of the origin, then the origin is unstable (Slotine and Li, 1991).

Substituting Eqs. (3), (9) and (A.4) into Eq. (A.3) gives

(i) when $\omega > 0$

$$\dot{V}_1(\theta, \omega) = \begin{cases} \omega\{-K_d\omega - T_d^+(\omega) + \tilde{T}_a - \tilde{T}_s^+\} & 0 < \theta \le \varepsilon_H \\ \text{undefined} & \theta = 0, \forall\theta \in \theta_n, \theta \notin S_1 \\ -\omega\{K_d\omega + T_d^+(\omega)\} & \text{otherwise} \end{cases} \tag{A.5a}$$

(ii) when $\omega < 0$

$$\dot{V}_1(\theta, \omega) = \begin{cases} \omega\{-K_d\omega - T_d^-(\omega) + \tilde{T}_s^- - \tilde{T}_s^+\} & \varepsilon_L \le \theta < 0 \\ \text{undefined} & \theta = 0, \forall\theta \in \theta_n, \theta \notin S_1 \\ -\omega\{K_d\omega + T_d^-(\omega)\} & \text{otherwise} \end{cases} \tag{A.5b}$$

From Eqs. (A.5a) and (A.5b), $\dot{V}_1(\theta, \omega)$ is positive definite in the region $P \equiv \{P^+ \cup P^-\}$ defined by

$$P^+ = \{(\theta, \omega) \in R^2 | 0 < \theta \le \varepsilon_H, \quad 0 < \omega < \omega^+\} \tag{A.6a}$$

$$P^- = \{(\theta, \omega) \in R^2 | \varepsilon_L \le \theta < 0, \quad \omega^- < \omega < 0\} \tag{A.6b}$$

where ω^+ and ω^- are determined from the first elements of Eqs. (A.5a) and (A.5b), and using Eq. (4)

$$\omega^+ = [\{\tilde{T}_s^+ - \tilde{T}_s^-\} - T_0^+]/(K_d + b_1) \tag{A.7a}$$

$$\omega^- = -[\{\tilde{T}_s^+ - \tilde{T}_s^-\} + T_0^-]/(K_d + b_1) \tag{A.7b}$$

Obviously, from the definitions of the friction parameters, ω^+ and ω^- are positive and negative, respectively. Thus P is not an empty set.

Since the region P is a neighborhood of the origin and the derivative is positive definite in P, the origin is unstable. Q.E.D.

Appendix B

Proof of Theorem 2. Choose the Lyapunov function candidate

$$V_2(\theta, \omega) = (1/2)J\omega^2 + g_2(\theta) \tag{B.1}$$

where the function $g_2(\theta)$ is defined as in Fig. 11 and as follows

$$g_2(\theta) = \begin{cases} \frac{1}{2} K_p(\theta^2 + \tilde{\theta}_H^2 - 2\tilde{\theta}_H\delta_H), & \tilde{\theta}_H < \theta \\ K_p\tilde{\theta}_H(\theta - \delta_H), & \delta_H < \theta \le \tilde{\theta}_H \\ 0 & \delta_L \le \theta \le \delta_H \\ K_p\tilde{\theta}_L(\theta - \delta_L) & \tilde{\theta}_L \le \theta < \delta_L \\ \frac{1}{2} K_p(\theta^2 + \tilde{\theta}_L^2 - 2\tilde{\theta}_L\delta_L) & \theta < \tilde{\theta}_L. \end{cases} \tag{B.2}$$

The function $V_2(\theta, \omega)$ is continuous w.r.t. θ and ω, and positive definite w.r.t. S_δ. If the time derivative of $V_2(\theta, \omega)$ is negative definite w.r.t. the region S_δ, then S_δ is asymptotically stable (Bhatia and Szego, 1970). The time derivative of $V_2(\theta, \omega)$ along the solution trajectories of the system has the discontinuity S_2 as discussed in Appendix C. From Eqs (B.1) and (B.2), the time derivative $\dot{V}_2(\theta, \omega)$ excluding the points in S_2 is given by

$$\dot{V}_2(\theta, \omega) = -K_d\omega^2 - \omega T_{slip}(\omega) + \omega\{g_2'(\theta) - T_n\} \tag{B.3}$$

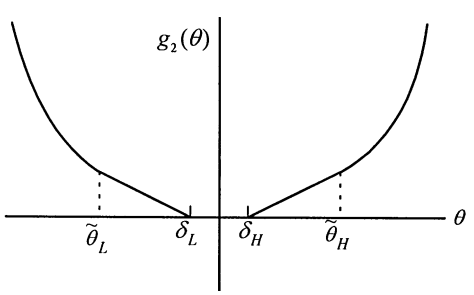

Fig. 11. Definition of the function $g_2(\theta)$.

where

$$g_2'(\theta) = \begin{cases} K_p\tilde{\theta}_H, & \delta_H < \theta \le \tilde{\theta}_H \\ 0, & \delta_L < \theta \le \delta_H \\ K_p\tilde{\theta}_L, & \tilde{\theta}_L \le \theta < \delta_L \\ K_p\theta, & \text{otherwise} \\ \text{undefined} & \theta = \delta_H, \theta = \delta_L \end{cases} \tag{B.4}$$

From Eqs. (12) and (B.4) the term $\omega\{g_2'(\theta) - T_n\}$ in Eq. (B.3) is reduced to

(i) when $\omega > 0$

$$\omega\{g_2'(\theta) - T_n\} = \begin{cases} \omega\tilde{T}_s^- & 0 < \theta \le \delta_H \\ \text{undefined} & \theta = \delta_H, \theta = \delta_L \\ 0 & \text{otherwise} \end{cases} \tag{B.5a}$$

(ii) when $\omega < 0$

$$\omega\{g_2'(\theta) - T_n\} = \begin{cases} \omega\tilde{T}_s^+ & \delta_L < \theta \le 0 \\ \text{undefined} & \theta = \delta_H, \theta = \delta_L \\ 0 & \text{otherwise.} \end{cases} \tag{B.5b}$$

Thus

$$\omega\{g_2'(\theta) - T_n\} \le 0, \quad \forall\{(\theta, \omega) | \theta \ne \delta_H, \delta_L\}. \tag{B.6}$$

From Eqs. (B.3) and (B.6), $\dot{V}_2(\theta, \omega)$ is negative semi-definite in the whole region outside S_3 $[\equiv \{S_2 \cup (\theta = \delta_H, \delta_L)\}]$. For the points in S_3, the Dini-derivative is considered instead of $\dot{V}_2(\theta, \omega)$ (Southward et al., 1991). All the discontinuities are simple; therefore the Dini-derivative is also negative semi-definite over the entire phase space. From Eq. (B.3), $\dot{V}_2(\theta, \omega)$ is identically zero in all points of θ-axis, and as discussed in the Appendix C only the trajectories which meet a point in S_δ are contained in this set; therefore S_δ is an asymptotically stable equilibrium region.

Appendix C

State trajectories of hysteresis control. Since the slip friction and the hysteresis compensator are discontinuous, the system, Eq. (1), has the surface of discontinuity S_2.

$$S_2 = \{(\theta, \omega) | (\theta\omega = 0)(\theta = \delta_H, \omega < 0) \cup (\theta = \delta_L, \omega > 0)\}$$

This surface S_2 divides the phase space into six regions and, as discussed by Southward et al. (1991), every trajectory leaves the region in a clokwise fashion, as shown in Fig. 12. The trajectories I-1 and I-2 are the representatives responses in the region S_2^1. The trajectory I-1 hits the θ-axis within $\delta_H < \theta < \tilde{\theta}_H$, and after that it passes into the open region S_2^2 through the discontinuous

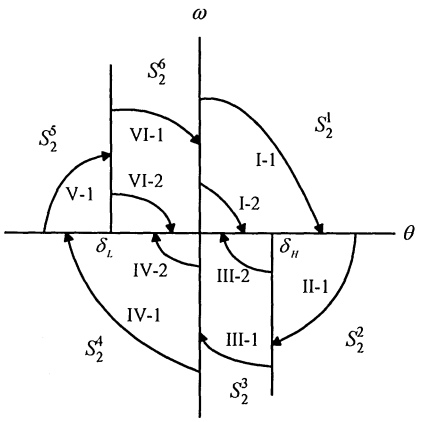

Fig. 12. Phase-plane response of the hysteresis control.

surface. On the other hand, the trajectory I-2 hits the θ-axis within $0 \leq \theta \leq \delta_H$, and then the control torque becomes zero according to Eq. (12c). Therefore the response stops at that point on the θ-axis. Similarly for the other regions, all the trajectories except those that do not hit the region S_δ pass from one open region through S_2 into the adjacent open region in a clockwise direction. Every trajectory that hits the region S_δ stops at the point of impact. Consequently, S_δ can be a set of equilibrium points.

References

Armstrong, B., Amin, B., 1996. PID Control in the presence of static friction: A comparison of algebraic and describing function analysis. Automatica, 32(5), 679–692.

Armstrong, B., Dupont, P., C. Canudas De Wit., 1994. A survey of models, analysis tools and compensation methods for control of machines with friction. Automatica, 30(7), 1083–1138.

Bhatia, N.P., Szego, G.P., 1970. Influence and partial compensation of simultaneously acting a backlash and Coulomb friction in position-and-controlled elastic two-mass systems of robots and machines tools. Inter. Conf. on Control and Applications, paper WA-4-5, IEEE, Jerusalem.

Canudas, C., Astrom, K.J., Braun, K., 1987. Adaptive friction compensation in DC-Motor Drives. IEEE J. of Robotics and Automation, R-3(6), 681–685.

Canudas, C., Olsson, H., Astrom, K.J., Lischinsky, 1995. A new model for control of systems with friction. IEEE Trans. on Automatic Control, 40(3), 419–425.

Dupont, P.E., 1994. Avoiding stick-slip through PD control. IEEE Trans. on Automatic Control, 39(5), 1094–1097.

Dupont, P.E., Dunlap, E.P., 1995. Friction modeling and PD compensation at very low velocities. ASME J. of Dynamic Systems, Measurement, and Control 117, 8–14.

Karnopp, D., 1985. Computer simulation of stick-slip friction in mechanical dynamic systems. ASME J. of Dynamic Systems, Measurement, and Control 107, 100–103.

Olsson, H., 1995. Describing function analysis of a system with friction. Proc. IEEE Conf. On Control Application, New York, pp. 310–315.

Radcliff, C.J., Southward, S.C., 1990. A property of stick-slip friction models which promotes limit cycle generation. Proc. 1990 American Control Conference, ACC, San Diego, pp. 1198–1203.

Southward, S.C., Radcliff, C.J., MacCluer, 1991. Robust nonlinear stick-slip friction compensation. ASME J. of Dynamic Systems, Measurement, and Control 113, 639–645.

Slotine, J.E., Li, W., 1988. Applied nonlinear control. Prentice Hall, pp. 117.

Yang, S., Tomizuka., 1988. Adaptive pulse width control for precise positioning under the influence of stiction and Coulomb friction. ASME J. of Dynamic Systems, Measurement, and Control 110, 221–227.